Intermittency and Conditional Averaging in a Turbulent Nonpremixed Flame by Raman Scattering

R. W. Pitz* and M. C. Drake†
General Electric Company, Schenectady, New York

Pulsed Raman scattering is used to determine zonal averages, intermittency, and conditional probability density functions (pdf's) for temperature, density, conserved scalar, and molecular composition in a turbulent, hydrogen jet diffusion flame. The conditional mean and rms values provide a data base for flame intermittency models. Both conventional and Favre-averaged turbulent zone pdf's of the conserved scalar are highly non-Gaussian in the intermittent regions. Turbulent combustion models that assume a clipped Gaussian turbulent pdf in this region could give erroneous results for flame processes sensitive to pdf shapes such as NO_x formation. Similar pdf shapes have been found in nonreacting wake flows and correlations obtained by Effelsberg and Peters using a three-zone (laminar, turbulent, and superlayer) model indicate that the superlayer can contribute up to 60% of the pdf.

Introduction

THE concept of intermittency and conditional (zonal) averaging has long been used by experimentalists to describe free turbulent flows and boundary layers.[1-5] This seems only natural as there exists in these flows turbulent and nonturbulent zones of fluid that have fundamentally different statistical properties. These flows are better understood when the turbulent and nonturbulent zones are separately analyzed by conditional averaging. Only in recent years have intermittency and conditional averaging been incorporated into turbulence models where the equations of motion are expressed separately for the turbulent and nonturbulent zones using conditional (zonal) averages and the intermittency is solved explicitly in a closed-form balance equation.[6-8]

In turbulent reacting flows (i.e., nonpremixed flames), the concept of intermittency and conditional averaging is seen to be even more important because of the highly nonlinear relationship between the mixture fraction (mass fraction of fuel) and the local thermodynamic state. Thus, although the local thermodynamic properties and gas composition can often be described by a single conserved scalar variable (the mixture fraction), the relationship between mixture fraction and the fluid composition, temperature, etc., is highly nonlinear, making average values of the temperature and fluid composition dependent on the statistical nature of the mixture fraction fluctuations. Combustion models generally overcome this nonlinear relationship by describing the fluctuations of the mixture fraction in terms of an assumed shape probability density function (pdf).[9] The degree of intermittency influences the pdf shape; it is not calculated directly, but has been empirically correlated by Kent and Bilger[10] from measurements in nonreacting flows. Measurements of intermittency and conditional averages in combusting flows are needed to check these correlations and assumed pdf shapes (Gaussian, beta function, etc.) and to provide data for more rigorous combustion models that solve for the intermittency directly and treat the turbulent and nonturbulent regions separately.

In this study, we present detailed pulsed Raman scattering measurements of intermittency in a turbulent ($Re=8500$), nonpremixed H_2 flame. Conditional analysis is used to determine pdf's, averages, and fluctuation values for temperature, density, and molecular composition in both turbulent and nonturbulent zones. The contribution of the viscous superlayer, a third zone between the turbulent and laminar zones, is calculated according to a correlation suggested by Effelsberg and Peters.[11]

Experimental

Raman measurements of conserved scalars and reactive scalars (temperature, mole fractions, etc.) and laser velocimetry measurements of axial velocity in the turbulent hydrogen jet diffusion flame have been presented elsewhere.[12-15] In this flame the hydrogen fuel flows from a 3.2 mm diameter tube that is centered in a coflowing airstream. The wind tunnel test section (1 m long) with a square cross section of 150×150 mm has four Pyrex windows (89×11.5 cm) to provide optical access. The fuel flow is metered by a calibrated critical flow nozzle. The measurements analyzed here were made in a turbulent jet diffusion flame of hydrogen with a Reynolds number, $Re=U_0d/\nu_0=8500$, where U_0 is the average cold-fuel flow velocity (285 m/s), d the jet diameter (3.2 mm), and ν_0 the kinematic viscosity of hydrogen at room temperature. The surrounding airstream velocity (with less than 0.2% free-stream turbulence) is 12.5 m/s, giving a velocity ratio of 23:1. The confined jet has an axial pressure gradient of -51 Pa/m. The Froude number of the jet (U_0^2/gd, where g is the gravitational acceleration) is 2.6×10^6, which indicates that the buoyancy effects are unimportant.

The Raman scattering apparatus is the same as described earlier[12,13] and only a few details are given here. A flashlamp-pumped dye laser tuned to 488 nm with a 0.2 nm bandwidth is triggered at 1 pulse/s, giving 1-2 J/pulse. The laser is focused into the jet flame and the Raman scattered light is collected at right angles and imaged onto the entrance slit of a ¾ m spectrometer. The spatial resolution defined by the spectrometer entrance slit, laser beam diameter, and collection optics magnification is $0.3\times0.3\times0.7$ mm. The temporal resolution of the measurement is 2 μs, which is the laser pulse length. Stokes vibrational Raman scattering from N_2, H_2O, H_2, and O_2 is detected to determine major species concentration. Since all the major species concentrations are

Presented as Paper 84-0197 at the AIAA 22nd Aerospace Sciences Meeting, Reno, NV, Jan. 9-12, 1984; received Jan. 4, 1985; revision received Aug. 19, 1985.

*Presently Assistant Professor, Department of Mechanical and Materials Engineering, Vanderbilt University, Nashville, TN. Member AIAA.

†Chemist, Corporate Research and Development. Member AIAA.

determined simultaneously, the measurement also gives total mass density, which permits either conventional averaging or density-weighted (Favre) averaging. The anti-Stokes vibration scattering from N_2 is also observed and, at temperatures greater than 800 K, the temperature is determined from the Stokes/anti-Stokes ratio. At temperatures less than 800 K, the temperature is calculated from the sum of the molecular species concentration using the ideal gas law.

Extensive calibration experiments in laminar premixed flames and uncertainty calculations based on photon counting statistics have been used to assess the precision and accuracy of the pulsed Raman measurements.[12] For temperature measurement, these studies have shown that the uncertainty in precision for a single temperature measurement is almost entirely due to photon counting statistics. The uncertainty in temperature measurement (in terms of relative standard deviation) is about $\pm 2\%$ at room temperature and about $\pm 4\%$ at flame temperatures. However, there are additional systematic errors in the temperature due to degradation of the dye laser pulse over the lifetime of the dye. These systematic errors are about ± 30 K at room temperature and ± 50 K at flame temperatures. For data sets of 2000 points, the uncertainty in the mean temperature is also about ± 50 K at flame temperatures, primarily due to these systematic errors as the random statistical errors are small.

In making "absolute" intensity measurements to determine mole fractions (and species concentrations), there are many sources of systematic error, such as beam defocusing. In a given set of measurements from one laser pulse, most of these systematic errors decrease all of the mole fraction (and concentration) values the same amount, such that the sum of the mole fractions adds up to ~ 0.95 instead of 1. All of the mole fraction and concentration values are divided by the measured sum of the mole fractions for each laser pulse measurement to correct for this systematic error. There are still some residual systematic errors and the precision of the individual mole fraction measurement is measured to be the larger of two values: either $\pm 8\%$ (relative standard deviation) or ± 0.01 in the mole fraction. These uncertainties are larger than expected from photon statistics.The uncertainty in the mean mole fractions of a 2000 point data set is limited by systematic errors to be the larger of two values: $\pm 5\%$ in the relative standard deviation or ± 0.005 in the mole fraction.

The measurements analyzed in this paper are at numerous radial positions and a single axial position of $x/d = 50$. The pulsed Raman results consist of 2000 independent single-laser shot measurements at each flame location (except at radial locations $r/R_\xi = 0.08$ and 1.33 where 200 measurements were recorded). Here, x is defined as the axial distance downstream of the jet nozzle, r the radial location from the jet center line, and R_ξ the radius at which the mixture fraction is half its centerline value.

The required spatial and temporal resolution for the experiments was determined by calculating the relevant turbulence length and time scales for the flame. The smallest length scale is the Kolmogorov length scale given by[16]

$$\eta = (\nu^3/\epsilon)^{1/4} \tag{1}$$

where ν is the kinematic viscosity. The viscosity is determined at each radial location using calculations for H_2/air mixtures by Bilger[17] and the measured local mean mixture fraction. The dissipation rate is approximated by[16]

$$\epsilon = u_{\text{rms}}^3/L \tag{2}$$

where u_{rms} is the axial rms velocity and L the integral length scale. The integral length scale has been measured in turbulent H_2/air diffusion flames by Stärner and Bilger[18] to be

$$L = 0.7R_u \tag{3}$$

where R_u is the radius at which the velocity is halfway between the centerline and freestream value.

The shortest time scale in the flame is the Kolmogorov time scale,

$$\tau_u = (\nu/\epsilon)^{1/2} \tag{4}$$

The velocities in the present flame were determined by laser velocimetry described elsewhere.[14] The velocity half-radius is $R_u = 10.8$ mm, which gives an integral scale of $L = 7.6$ mm. The radial positions are normalized by the measured half-radius of the conventionally averaged mixture fraction, R_ξ ($R_\xi = 10.6$ mm at $x/d = 50$).

The Kolmogorov length and time scales in our flame are summarized in Table 1. Others[19] have stated that in turbulent flames the measurement spatial and time resolution are adequate if they are less than ~ 3 times the Kolmogorov scales. The Raman time resolution (2 μs) is well within this requirement. The measurement spatial resolution ($0.6 \times 0.3 \times 0.3$ mm) is adequate as the longest dimension is about 3η.

Also listed in Table 1 are the turbulence Reynolds numbers based upon the integral length scale,

$$Re_L = u_{\text{rms}} L/\nu \tag{5}$$

and based upon the Taylor microscale,[16]

$$Re_\lambda = u_{\text{rms}}\lambda/\nu \cong (15R_L)^{1/2} \tag{6}$$

where λ is the Taylor microscale. For nonreacting flows, Saffman[20] suggests that R_λ needs to exceed approximately 100 to represent fully turbulent flow. Our values in reacting flows are 40-50 and are below Saffman's estimate for nonreacting flow. However, our turbulence levels are comparable to other reacting coflowing jets at higher Reynolds numbers. For instance, the centerline turbulence levels from a hydrogen/air coflowing jet ($Re = 11{,}000$) studied by Stärner and Bilger[18] and from a hydrogen/argon/air coflowing jet ($Re = 24{,}000$) studied by Driscoll et al.[21] are similar to our $Re = 8500$ data as shown in Fig. 6b of Ref. 14.

Results

For intermittency and conditional averaging measurements, the discrimination between turbulent and nonturbulent fluid should conceptually rely on the variance of the vorticity fluctuations, but vorticity is very difficult to measure. However, since the airstream is initially laminar and the hydrogen jet is initially turbulent, the presence of significant hydrogen-bearing species from the fuel is used to identify turbulent zones. Limited results of intermittency and conditional means, rms values, and pdf's have been presented earlier that were based on the sum of $X_{H_2O} + X_{H_2}$ as the discriminating function.[15,22] The much more detailed results presented here are conditioned on the conserved scalar mixture fraction, which is more rigorous. The mixture fraction (the hydrogen elemental mass fraction) is given by

Table 1 Fluid mechanical scales

r/R_ξ	U, m/s	u_{rms}, m/s	$\nu \times 10^4$, m^2/s	$\epsilon \times 10^{-3}$, m^2/s^3	η, mm	τ_u, μs	Re_L	Re_λ
0.08	47.4	6.8	3.08	40.0	0.16	90	170	50
0.84	34.5	6.8	3.50	40.0	0.18	90	150	50
1.03	30.3	6.3	3.71	32.0	0.20	110	130	45
1.22	26.4	6.5	3.95	35.0	0.20	110	130	45
1.33	23.0	5.8	4.12	25.0	0.23	130	110	40
1.41	21.2	5.8	4.05	25.0	0.23	130	110	40
1.59	15.4	3.1	2.37	3.8	0.24	250	100	40
1.78	13.7	1.5	1.12	0.47	0.23	500	110	40
1.97	13.3	0.6	0.460	0.028	0.24	1300	100	40

$$\xi = \frac{[2.016(C_{H_2} + C_{H_2O})/\rho] - Z_{H,a}}{1 - Z_{H,a}} \tag{7}$$

where

$$Z_{H,a} = \frac{2.016}{18.016}\left(\frac{\omega}{1+\omega}\right) \tag{8}$$

where C_{H_2} and C_{H_2O} are the molar concentrations of H_2 and H_2O, ρ the density, and ω the specific humidity (kg H_2O/kg dry air) in the inlet air. The humidity was measured directly from frequent Raman calibration measurements in room air and from a hygrometer. The stoichiometric value of ξ is 0.0283.

In this study, the flow is considered turbulent when $\xi \geq 0.0004$ and nonturbulent when $\xi < 0.0004$. The threshold level was determined by analyzing the conditional pdf's of temperature. A typical conditional pdf of the temperature in the intermittent layer of the jet is shown in Fig. 1a. The probability scale in all of the pdf's are normalized so that the in-

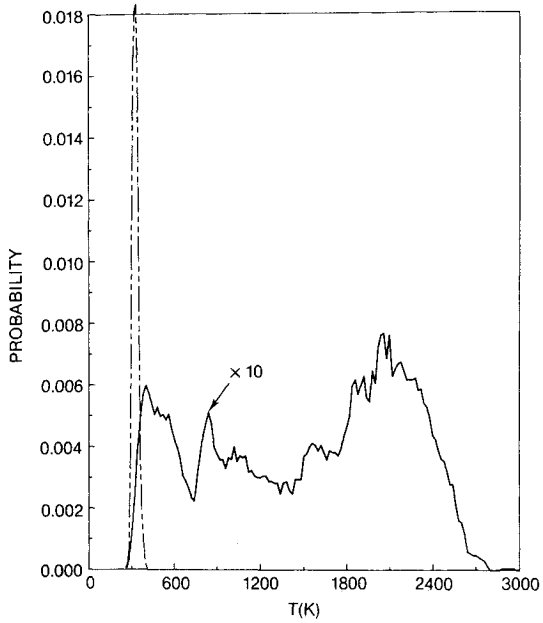

a) Full pdf ($\bar{\gamma} = 0.86$, — turbulent, ------ nonturbulent).

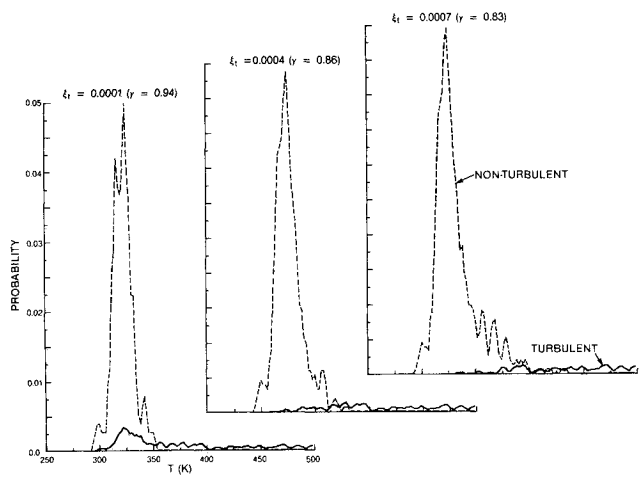

b) Intermittent spike region as a function of threshold setting (— turbulent, ---- nonturbulent).

Fig. 1 Conditional probability density function of temperature ($Re = 8500$, $x/d = 50$, $r/R_\xi = 1.6$).

Table 2 Conditional averages from Raman data at the same flame conditions given in Fig. 1a

Condition	Turbulent fluid	Nonturbulent fluid	All
T, K	1520	330	1350
T', K	680	13	760
X (N_2)	0.69	0.78	0.70
X' (N_2)	0.08	0.01	0.08
X (H_2O)	0.19	0.01	0.16
X' (H_2O)	0.12	0.002	0.12
X (H_2)	0.02	—	0.02
X' (H_2)	0.05	—	0.05
X (O_2)	0.09	0.20	0.11
X' (O_2)	0.07	0.01	0.08
ρ, kg/m^3	0.30	1.08	0.41
ρ', kg/m^3	0.23	0.04	0.35
ξ	0.017	0.0001	0.015
ξ'	0.014	0.0001	0.014
$\tilde{\xi}$	0.009	0.0001	0.006
ξ''	0.011	0.0001	0.010
γ	0.86		
$\tilde{\gamma}$	0.63		

Note: All averages are conventional, except those denoted by (~) which are Favre mean averages and (″) which are Favre rms averages. Conventional rms averages are denoted by (′).

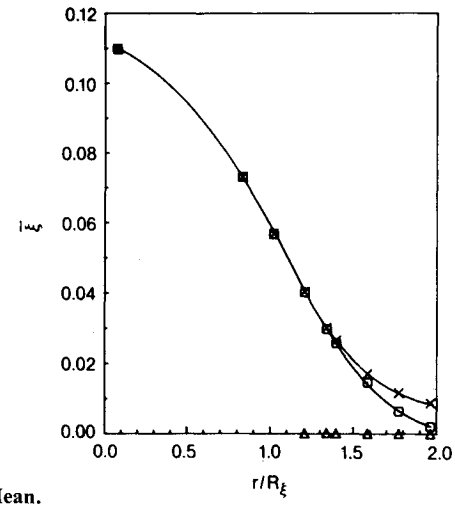

a) Mean.

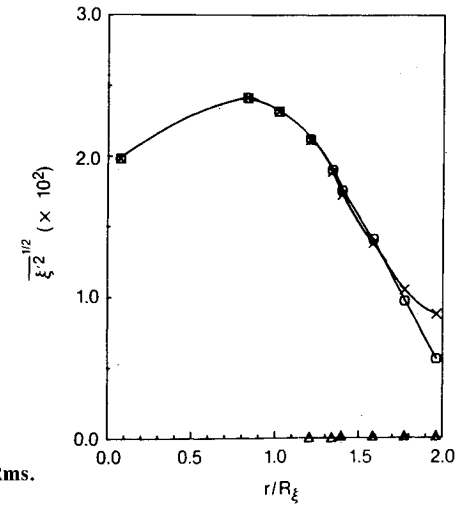

b) Rms.

Fig. 2 Conditional mixture fraction ($x/d = 50$, △: nonturbulent, ×: turbulent, □: average).

tegral of each of the conditional pdf's is one. An expanded view of the intermittent spike region is shown in Fig. 1b for different threshold settings. Only the cold temperature regions are shown. The shapes of the nonturbulent spike and the cold tail of the turbulent pdf were found to be very sensitive to the threshold setting due to the large temperature differences (over 1000 K) between the two zones. When the threshold setting ξ_t was too low ($\xi_t = 0.0001$ in Fig. 1b), a cold spike appeared in the turbulent pdf. For too high a threshold setting ($\xi_t = 0.0007$ in Fig. 1b), the nonturbulent spike was skewed to the high-temperature side. Conditional pdf's were plotted at 0.0001 mixture fracton intervals for measurements made at many different flame positions and the threshold was determined to be $\xi_t = 0.0004 \pm 0.0001$ by analyzing the pdf shape in the intermittent spike region. This level was constant for all of the data analyzed. The uncertainty of ± 0.0001 results primarily from the ± 0.002 uncertainty in the measurements of the mole fraction of water in the air. As seen in Fig. 1b, the selection of the threshold setting does effect the intermittency determination. The ± 0.0001 variation in the threshold setting corresponds to at most a ± 0.02 variation in the calculated value of intermittency.

The pdf's, zonal averages, and higher moments can be determined directly from the Raman data. For example, the conditionally averaged pdf of temperature shown in Fig. 1a is from 2000 independent measurements in the $Re = 8500$ H_2 flame at $x/d = 50$ and $r/R_\xi = 1.6$. The nonturbulent fluid shows a narrow spike at room temperature and the turbulent fluid shows a broad non-Gaussian pdf.

The conditionally averaged mean and rms values for the same data are given in Table 2. The turbulent and nonturbulent fluids show markedly different mean (and rms) values for temperature, density, and composition. The nonturbulent fluid has the mean properties of room air and very low rms values. Plots of conditional mean and rms averages for ξ, $\tilde{\xi}$, T, ρ, X_{H_2}, X_{H_2O}, X_{O_2} and X_{N_2} are shown in Figs. 2-9 for many radial positions across the flame at $x/d = 50$. In the nonturbulent zones, the mean values are equal to room air values (within the experimental error of ± 30 K and ± 0.01 mole fraction) and the rms values are small. In the turbulent zones, the mean values show a large radial variation (except for density and oxygen mole fraction) and the rms values are large.

The constant-density region in the center of the jet (Fig. 5a) is simply a result of equilibrium thermodynamic considerations. The equilibrium density is shown as a function of mixture fraction in Fig. 10 and only varies $\pm 7\%$ for the mixture fraction range 0.04-0.14. Schefer and Dibble[23] found the same constant density region in H_2/Ar jet flames from conditional analysis of Rayleigh scattering measurements.

The mean temperature and $\bar{X}_{H_2O}$ profiles both peak near the time averaged flame front position ($r/R_\xi \cong 1.3$), which is the point where the average mixture fraction equals its stoichiometric value (0.0283). The turbulent zone rms averages generally peak farther out in the outer shear layer ($r/R_\xi \cong 1.6$) where the Favre intermittency $\tilde{\gamma}$ is about 0.5 (see the intermittency values in Fig. 11). The exceptions are $(\overline{\xi''^2})^{1/2}$, $(\overline{\tilde{\xi}''^2})^{1/2}$ and $(\overline{X'^2_{H_2}})^{1/2}$, which peak on the rich side

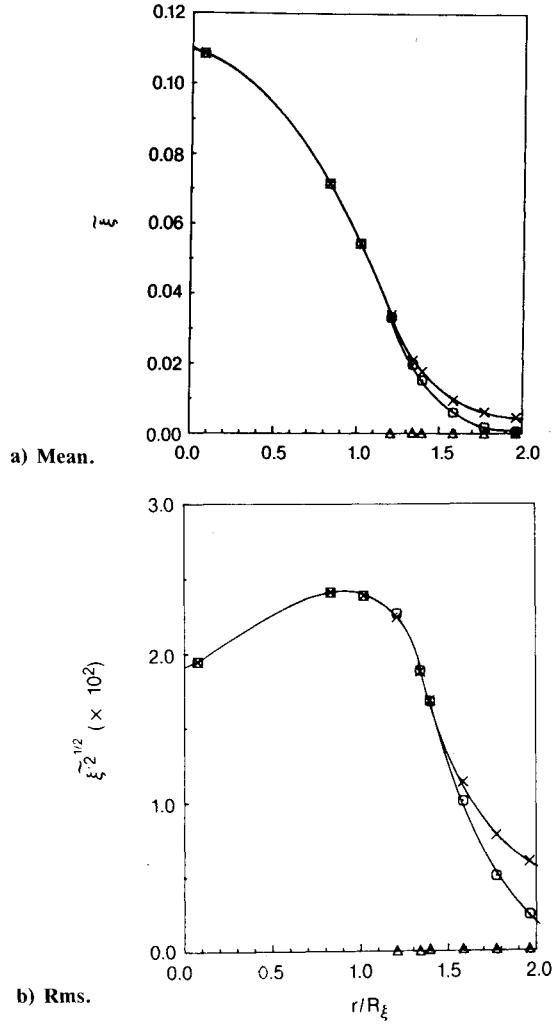

Fig. 3 Conditional Favre mixture fraction (same conditions as Fig. 2).

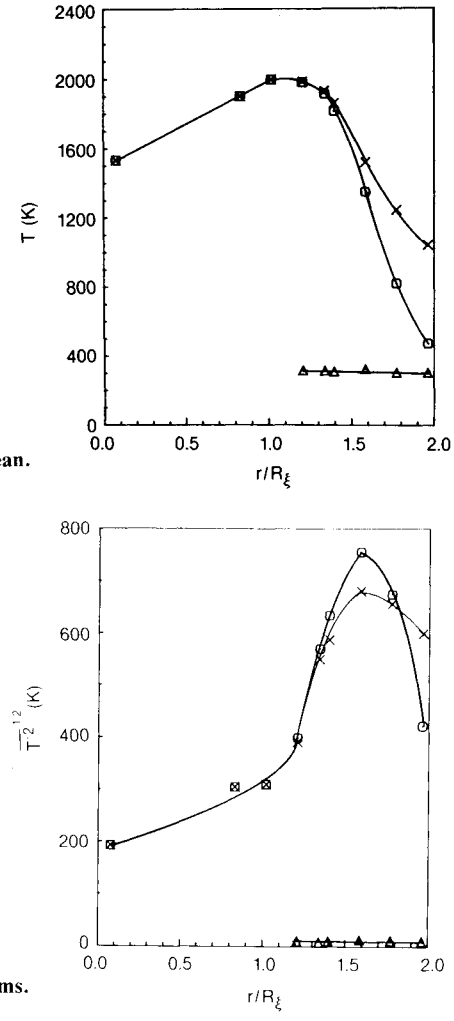

Fig. 4 Conditional temperature (same conditions as Fig. 2).

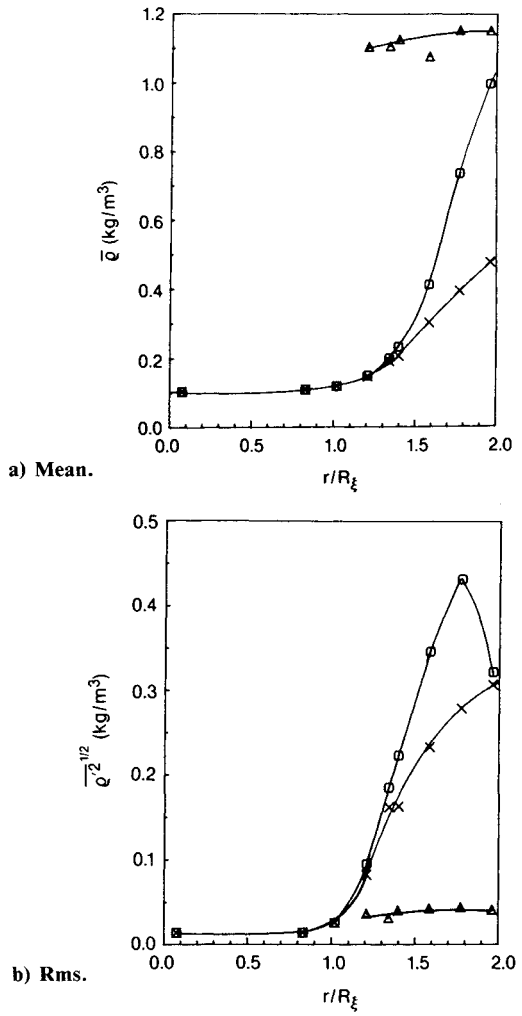

Fig. 5 Conditional density (same conditions as Fig. 2).

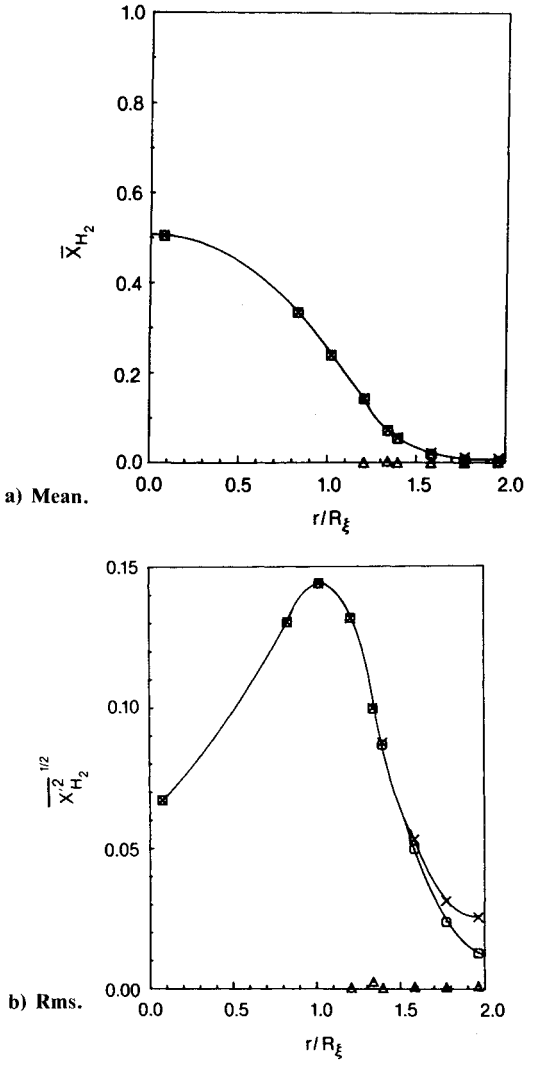

Fig. 6 Conditional X_{H_2} (same conditions as Fig. 2).

($r/R_\xi = 1.0$), and $(\overline{\rho'^2})^{1/2}$, which peaks on the lean side $r/R_\xi = 1.8$. In all cases, the turbulent rms values are generally less than the total average rms until the intermittency $\bar{\gamma}$ drops below 0.5 at $r/R_\xi \cong 1.8$ and then the turbulent rms values are greater.

The pdf's of conventionally averaged mixture fraction are shown in Fig. 11, where the intermittency values have been calculated according to the analysis discussed earlier. The pdf's look Gaussian in the center, but as soon as there is any significant intermittency, the turbulent pdf's appear non-Gaussian. This is seen more clearly by analyzing the turbulent zone pdf's of mixture fraction shown in Figs. 12 and 13. The conventional pdf's in these figures show non-Gaussian (positively skewed) shapes, even though the intermittency values are close to one ($\bar{\gamma} = 0.97$ in Fig. 12). Farther out in the intermittent region, the conventional pdf's are even more positively skewed and non-Gaussian.

The Favre pdf's shown in Figs. 12 and 13 are more non-Gaussian than the conventional pdf's. The Favre pdf's are calculated by density weighting the conventional pdf (see Bilger[9]). With Raman scattering, both the density and mixture fraction are determined simultaneously and the measured density values are used to weight the conventional pdf. Since the density in H_2/air flames is close to equilibrium, the conventional pdf's are essentially weighted by the density vs mixture fraction variation shown in Fig. 10. In the center of the jet where the conventional pdf's are Gaussian and the mixture fraction values are always high ($\xi > 0.02$), the density weighting leaves the pdf shape unchanged. However, as seen in Figs. 12 and 13, when the mixture fraction values are low ($\xi < 0.02$), the density weighting strongly skews the conventional pdf. Further from the jet centerline at $r/R_\xi = 1.8$ and 2.0 (not shown here) where the intermittency is lower ($\bar{\gamma} = 0.55$ and 0.23), both the Favre and conventional turbulent pdf's are even more strongly skewed.

Thus, both the Favre and conventional turbulent pdf's of conserved scalar show considerable non-Gaussian behavior in the intermittent zones of the flame. The assumption of a clipped Gaussian shape for the pdf of mixture fraction (often made in combustion models) does not seem justified. Prediction of processes that depend on the assumed pdf shape, such as NO_x formation, may be in error if a Gaussian shape is assumed. The exponential dependence of NO formation on temperature makes its production very sensitive to the mixture fraction variations. Kent and Bilger[10] studied the effect of pdf shape on NO production in H_2/air turbulent jet flames. By varying the assumed shape of the mixture fraction pdf from a clipped Gaussian to a positively skewed pdf, they found approximately a factor of two difference in NO production rate and concluded that "nitric oxide concentrations are found to be particularly sensitive to the form of the probability density function indicating that the measurement of pdf's in flames is an important area for further work." The strong non-Gaussian effects found in this work should be taken into account when modeling NO production in turbulent flames.

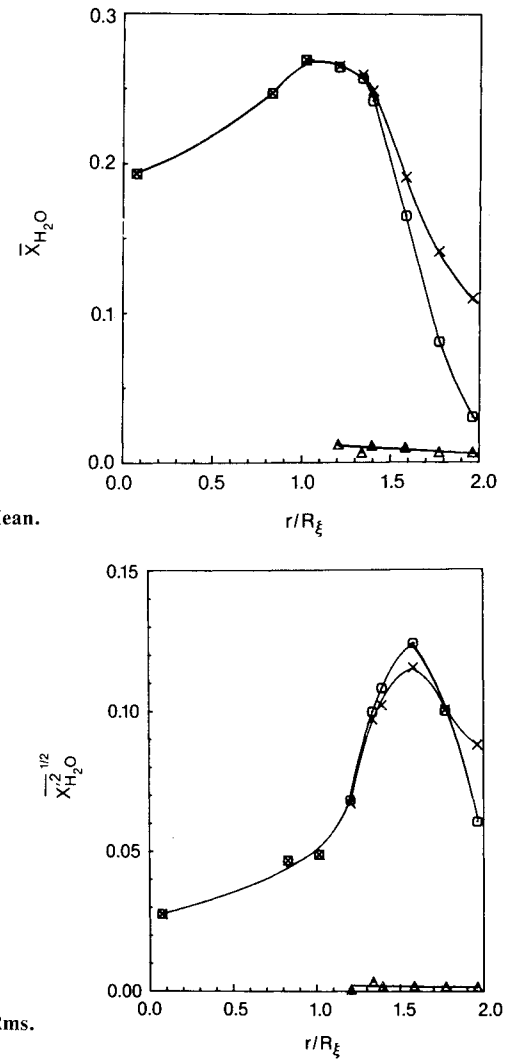

Fig. 7 Conditional X_{H_2O} (same conditions as Fig. 2).

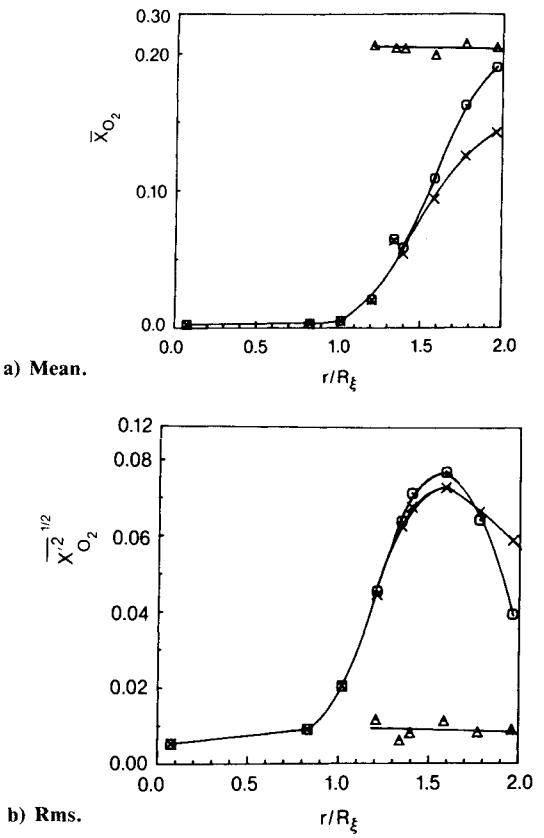

Fig. 8 Conditional X_{O_2} (same conditions as Fig. 2).

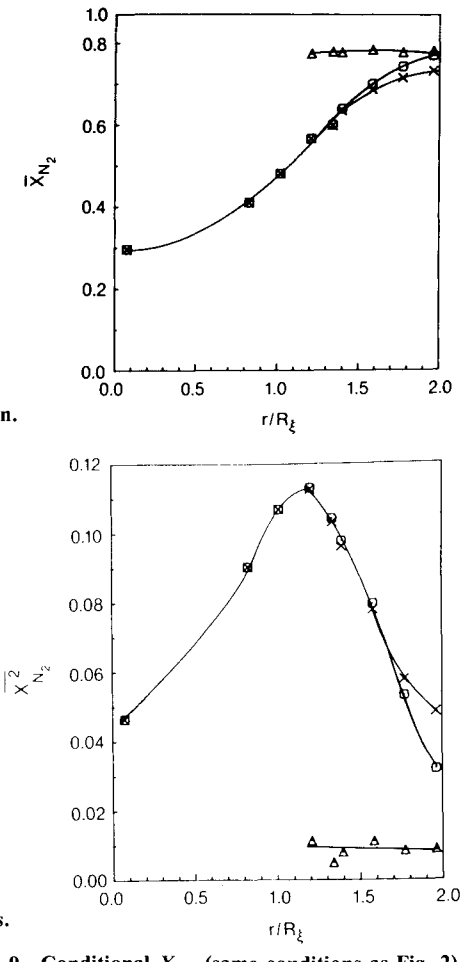

Fig. 9 Conditional X_{N_2} (same conditions as Fig. 2).

Bilger[9] has attributed the triangular shape of the turbulent pdf (Figs. 12 and 13) in the intermittent region to the presence of the viscous superlayer—a viscous layer between the turbulent and nonturbulent zones first discussed by Corrsin.[1] Effelsberg and Peters[11] have recently proposed an empirical pdf model for the conserved scalar pdf that seeks to quantify the viscous superlayer effects. Their empirical model separates the pdf's into three zones (fully turbulent, superlayer, and laminar) and relates the zonal probabilities to the first four moments of the mixture fraction distribution.

Analyzing pdf's from nonreacting turbulent wakes,[24] Effelsberg and Peters have correlated the superlayer portion of the turbulent pdf to the intermittency giving the probability of a superlayer as

$$P_{SL} = \bar{\gamma} S \tag{9}$$

where

$$S = (1 - \bar{\gamma}^2)^{1/4} \tag{10}$$

The probabilities of the nonturbulent and turbulent zones are

$$P_{NT} = 1 - \bar{\gamma} \tag{11}$$

$$P_T = \bar{\gamma}(1 - S) \tag{12}$$

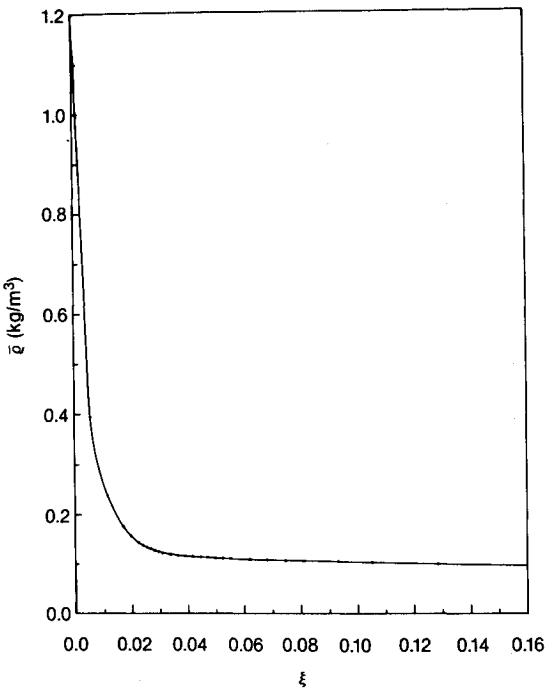

Fig. 10 Adiabatic equilibrium density dependence on the mixture fraction for hydrogen/air combustion (initial pressure and temperature: 1 atm, 298 K).

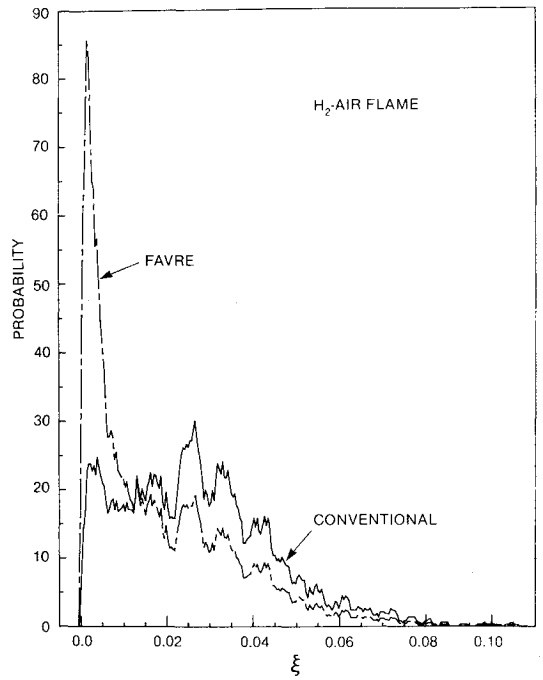

Fig. 12 Conditional (turbulent fluid only) probability density function of mixture fraction ($Re = 8500$, $x/d = 50$, $r/R_\xi = 1.4$, $\bar{\gamma} = 0.97$, — conventional probability, —·— Favre probability).

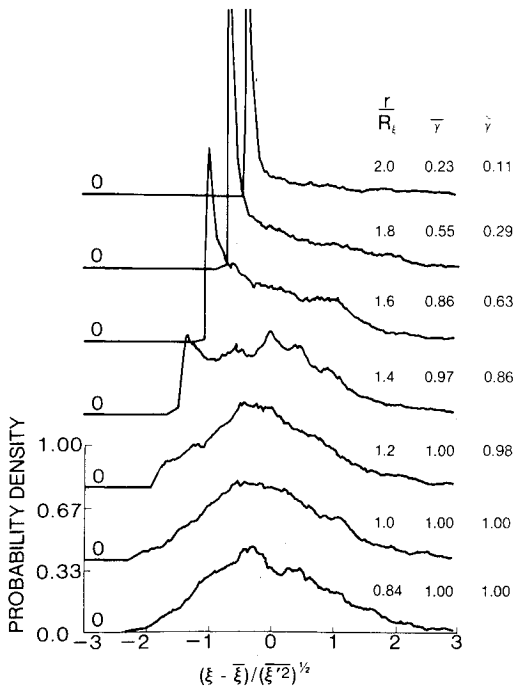

Fig. 11 Probability density functions of mixture fraction ($Re = 8500$, $x/d = 50$; note zero shift in curves).

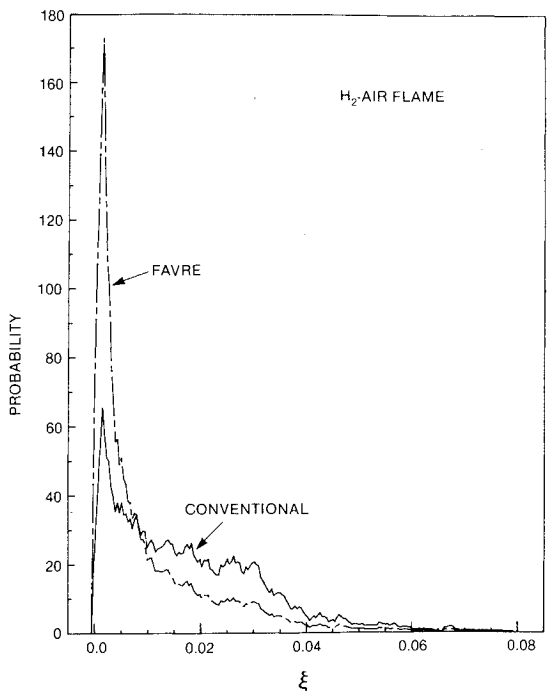

Fig. 13 Conditional (turbulent fluid only) probability density function of mixture fraction ($Re = 8500$, $x/d = 50$, $r/R_\xi = 1.6$, $\bar{\gamma} = 0.86$, — conventional probability, —·— Favre probability).

Mixture fraction pdf's measured here in turbulent jet diffusion flames (such as seen in Figs. 12 and 13) are shaped similarly to the pdf's from nonreacting wake flows that Effelsberg and Peters analyzed. Applying the same correlation to our data in the turbulent flame gives the probability of the three zones as shown in Fig. 14. The probability of superlayer is symmetric and peaks at the same position where the rms values (both turbulent and total) are maximum ($r/R_\xi = 1.6$). This is outside of the average flame front position ($r/R_\xi = 1.3$). The very high probability of the superlayer (0.6) indicates that the superlayer is equally important in turbulent jet diffusion flames as it is in nonreacting wake flows.

Finally, because the pulsed Raman data provide such a detailed instantaneous analysis of the state of the fluid, many other forms of conditional sampling become feasible. For example, pdf's and moments can be conditioned on whether the sample is in a rich or lean zone of the flame. Conditioning on rich or lean zones may be important for analysis of flame kinetic processes such as NO_x pollutant formation from "prompt" NO,[25] which occurs only in rich flame zones.

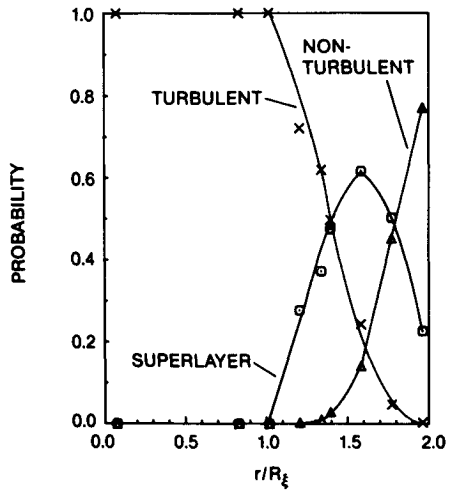

Fig. 14 Three zone probability based on correlation by Effelsberg and Peters[11] (×: turbulent, □: superlayer, △: nonturbulent).

Conclusions

Pulsed Raman scattering is found to be a powerful technique for measuring intermittency, zonal pdf's, zonal averages, and higher conditional moments in turbulent reacting flows because it provides simultaneous measurements of temperature, density, mixture fraction, and major species mole fractions. Such a complete description of the thermodynamic state of turbulent flame zones is not presently possible with any other techniques. The technique gives very good time resolution and adequate spatial resolution when compared to the fluid mechanical scales in this turbulent H_2 air flame. Its major limitation is a relatively slow data rate (1-10 s^{-1}), which limits the size of data samples obtainable. Zonal pdf's, averages, and higher moments have been determined and provide a data base for comparison to flame intermittency models. The nonturbulent fluid has constant mean values equal to those in room air and small rms fluctuating values. The turbulent fluid has a much larger radial variation in its average and rms values. Conditional pdf's of mixture fraction (both conventional and Favre) in the intermittent layer show a turbulent pdf that is non-Gaussian, exhibiting a large contribution attributed to the superlayer zone. These non-Gaussian turbulent pdf shapes should be taken into account in computational codes that model processes sensitive to pdf shape, such as NO_x formation. Preliminary data comparisons to a three-zone model by Effelsberg and Peters provide support for an extensive superlayer zone.

Acknowledgments

The authors gratefully acknowledge the expert experimental and analytical support of Frank Haller and the pioneering work of Marshall Lapp and Murray Penney on the development of pulsed Raman scattering.

References

[1]Corrsin, S. and Kistler, A. L., "Free-stream Boundaries of Turbulent Flows," NACA Rept. 1244, 1955.

[2]Wygnanski, I. and Fiedler, H. E., "The Two-Dimensional Mixing Region," *Journal of Fluid Mechanics*, Vol. 41, 1970, pp. 327-361.

[3]Antonia, R. A., Prabhu, A., and Stephenson, S. E., "Conditionally Sampled Measurements in a Heated Turbulent Jet," *Journal of Fluid Mechanics*, Vol. 72, 1975, pp. 455-480.

[4]Demetriades, A., "Turbulent Front Structure of an Axisymmetric Compressible Wake," *Journal of Fluid Mechanics*, Vol. 34, 1968, pp. 465-480.

[5]Libby, P. A., Chigier, N., and LaRue, J. C., "Conditional Sampling in Turbulent Combustion," *Progress in Energy and Combustion Science*, Vol. 8, 1982, pp. 203-231.

[6]Libby, P. A., "Prediction of the Intermittent Turbulent Wake of a Heated Cylinder," *The Physics of Fluids*, Vol. 19, 1976, pp. 494-501.

[7]Byggstøyl, S. and Kollmann, W., "Closure Model for Intermittent Turbulent Flows," *International Journal of Heat and Mass Transfer*, Vol. 24, 1981, pp. 1811-1822.

[8]Kollmann, W., "The Prediction of the Intermittency Factor for Turbulent Shear Flows," *AIAA Journal*, Vol. 22, 1984, pp. 486-492.

[9]Bilger, R. W., "Turbulent Flows with Nonpremixed Reactants," *Turbulent Reacting Flows*, edited by P. A. Libby and F. A. Williams, Springer-Verlag, New York, 1980, pp. 65-113.

[10]Kent, J. H. and Bilger, R. W., "The Prediction of Turbulent Diffusion Flame Fields and Nitric Oxide Formation," *Sixteenth Symposium (International) on Combustion*, The Combustion Institute, Pittsburgh, PA, 1977, pp. 1643-1656.

[11]Effelsberg, E. and Peters, N., "A Composite Model for the Conserved Scalar PDF," *Combustion and Flame*, Vol. 50, 1983, pp. 351-360.

[12]Drake, M. C., Lapp, M., and Penney, C. M., "Use of the Vibrational Raman Effect for Gas Temperature Measurements," *Temperature: Its Measurement and Control in Science and Industry*, Vol. 5, edited by J. F. Schooley, American Institute of Physics, New York, 1982, pp. 631-638.

[13]Drake, M. C., Lapp, M., Penney, C. M., Warshaw, S., and Gerhold, B. W., "Measurements of Temperature and Concentration Fluctuations in Turbulent Diffusion Flames Using Pulsed Raman Spectroscopy," *Eighteenth Symposium (International) on Combustion*, The Combustion Institute, Pittsburgh, PA, 1981, pp. 1521-1531.

[14]Drake, M. C., Pitz, R. W., and Lapp, M., "Laser Measurements on Nonpremixed H_2-Air Flames for Assessment of Turbulent Combustion Models," *AIAA Journal*, to be published.

[15]Drake, M. C., Bilger, R. W., and Stärner, S. H., "Raman Measurements and Conserved Scalar Modeling in Turbulent Diffusion Flames," *Nineteenth Symposium (International) on Combustion*, The Combustion Institute, Pittsburgh, PA, 1982, pp. 459-467.

[16]Tennekes, H. and Lumley, J. L., *A First Course in Turbulence*, MIT Press, Cambridge, MA, 1972.

[17]Bilger, R. W., "Molecular Transport Effects in Turbulent Diffusion Flames at Moderate Reynolds Number," *AIAA Journal*, Vol. 20, 1982, pp. 962-970.

[18]Stärner, S. H. and Bilger, R. W., "LDA Measurements in a Turbulent Diffusion Flame with Axial Pressure Gradient," *Combustion Science and Technology*, Vol. 21, 1980, pp. 259-276.

[19]Goulard, R., Mellor, A. M., and Bilger, R. W., "Combustion Measurements in Air Breathing Propulsion Engines. Survey and Research Needs," *Combustion Science and Technology*, Vol. 14, 1976, pp. 195-219.

[20]Saffman, P. G., "Problems and Progress in the Theory of Turbulence," *Structure and Mechanisms of Turbulence*, Vol. II, edited by H. Fiedler, *Lecture Notes in Physics*, Vol. 76, Springer-Verlag, New York, 1978, p. 278.

[21]Driscoll, J. F., Schefer, R. W., and Dibble, R. W., "Mass Fluxes $\rho'u'$ and $\rho'v'$ Measured in a Turbulent Nonpremixed Flame," *Nineteenth Symposium (International) on Combustion*, The Combustion Institute, Pittsburgh, PA, 1982, pp. 477-485.

[22]Drake, M. C., Lapp, M., Pitz, R. W., and Penney, C. M., "Dynamic Measurements of Gas Properties by Vibrational Raman Scattering: Application to Flames," *Time Resolved-Vibrational Spectroscopy*, edited by G. H. Atkinson, Academic Press, New York, 1983, pp. 83-90.

[23]Schefer, R. W. and Dibble, R. W., "Simultaneous Measurements of Velocity and Density in a Turbulent Nonpremixed Flame," *AIAA Journal*, Vol. 23, 1985, pp. 1070-1078.

[24]LaRue, J. C. and Libby, P. A., "Temperature Fluctuations in a Plane Turbulent Wake," *The Physics of Fluids*, Vol. 17, 1974, pp. 1956-1967.

[25]Hayhurst, A. N. and Vince, I. M., "The Origin and Nature of 'Prompt' Nitric Oxide in Flames," *Combustion and Flame*, Vol. 50, 1983, pp. 41-57.